Chapter 19

One-Dimensional Titanium Dioxide and Its Application for Photovoltaic Devices

Norani Muti Mohammed, Robabeh Bashiri, Suriati Sufian, Chong Fai Kait and Saeed Majidai

Additional information is available at the end of the chapter

http://dx.doi.org/10.5772/intechopen.72976

Abstract

One-dimensional (1D) TiO_2 nanostructures (e.g., nanotubes, nanobelts, nanowires, and nanorods) have been considered to be very attractive candidates for various applications including photocatalytic degradation of pollutants, photocatalytic CO_2 reduction into energy fuels, water splitting, solar cells, supercapacitors, and lithium-ion batteries. More importantly, the dimensionality associated with zero-dimensional TiO_2 nanostructures gives unique physical properties, including a high aspect ratio structure, chemical stability, excellent electronic or ionic charge transfer, and a specific interface effect. This chapter elaborates on crystal structure and properties, preparation techniques, strategies for improving photocatalytic activity of 1D-TiO_2 nanostructure and its applications. Amongst all preparation techniques, the influence of experimental parameters on morphologies of 1D-TiO_2 nanostructure using hydro/solvothermal method is extensively explained. Furthermore, some critical engineering strategies to enhance the properties of 1D-TiO_2 nanostructures like increasing the surface area, extending the light absorption, and efficient separation of electrons/holes that advantage their potential applications are described. Moreover, a brief summary of their environmental and energy applications is provided.

Keywords: TiO_2, photocatalyst, one dimensional, hydrothermal, nanorod, nanobelts

1. Introduction

The wide applications of titanium dioxide, such as pigments, sunscreen, paints, and various commercialize applications correspond to its profound optical refractive ability, chemical stability, and low toxicity. Furthermore, TiO_2 has been extensively investigated as one of the most promising materials in photovoltaic devices, photocatalysis, photodegradation,

energy storage, and electrochromic devices. This is being established when the photoelectrolysis of water into H_2 and O_2 was reported under UV irradiation of the solar spectrum over the surface of TiO_2 photoelectrode in the photoelectrochemical (PEC) cell by Fujishima and Honda. In recent years, 1D-TiO_2 nanostructures have been significantly studied due to its distinctive advantages with regard to less charge carrier recombination rate and unique physical and chemical properties [1, 2]. In general, 1D nanostructures are well-known for their high aspect ratio in which at least one of its dimensions should be in the range of 1–100 nm regardless of their shapes such as rod, wire, belt or tube. The properties of one-dimensional single crystalline Ti-O-based nanomaterials are comparable with titania nanoparticles not only inherit almost all typical features of the nanoparticles, but also illustrate some new properties and improved performance in specific area [1]. It can afford direct transport pathways for charge carriers, decouple the direction for light absorption, and charge carrier transportation. Moreover, 1D semiconductor nanostructures are able to facilitate the light absorption and scattering, which is beneficial for photocatalytic reactions.

However, wide applications of 1D-TiO_2 nanostructures are diminished due to absorption of small portion of solar spectrum, relatively low specific surface area, and presence of single phase that pose certain limitations for it performance [3]. Several published research works have illustrated that well designed 1D-TiO_2 nanostructures play a significant role to overcome the above-mentioned problem, preserve the intrinsic characteristics of TiO_2, and finally the material with some new properties. In recent years, breakthroughs have continually been made in the preparation, modification, and applications of 1D-TiO_2 nanomaterials. In this chapter, we would like to address the crystal structure of TiO_2 and various synthesis process of 1D-TiO_2 nanostructured materials. Then, we will look into some critical structure engineering strategies that give 1D-TiO_2 nanostructured materials excellent properties for various applications.

2. Crystal structure and properties of 1D-TiO_2 nanostructure

TiO_2 is typically the *n*-type photocatalyst due to oxygen deficiency. Anatase (tetragonal, a = b = 3.782 Å, c = 9.502 Å), rutile (tetragonal, a = b = 4.584 Å, c = 2.953 Å), and brookite (rhombohedral, a = 5.436 Å, b = 9.166 Å, c = 5.135 Å) are three different crystalline polymorphs of TiO_2 [4]. **Figure 1a–c** shows that all these phases are constructed by connecting Ti—O octahedrons through a variable number of shared corners, and/or faces.

Figure 1a reveals that tetragonal structure of anatase is the result of corner (vertices) sharing octahedron which form (001) planes. In rutile structure, sharing edges of octahedrons at (001) planes give the tetragonal structure as shown in **Figure 1b**. While an orthorhombic structure of Brookite is the result of sharing both edges and corners of octahedrons [5, 6]. Rutile is the most stable crystal phase of TiO_2 while anatase is a metastable phase, which can be transformed to thermodynamically stable rutile over calcination temperature exceeding ~600°C [7, 8].

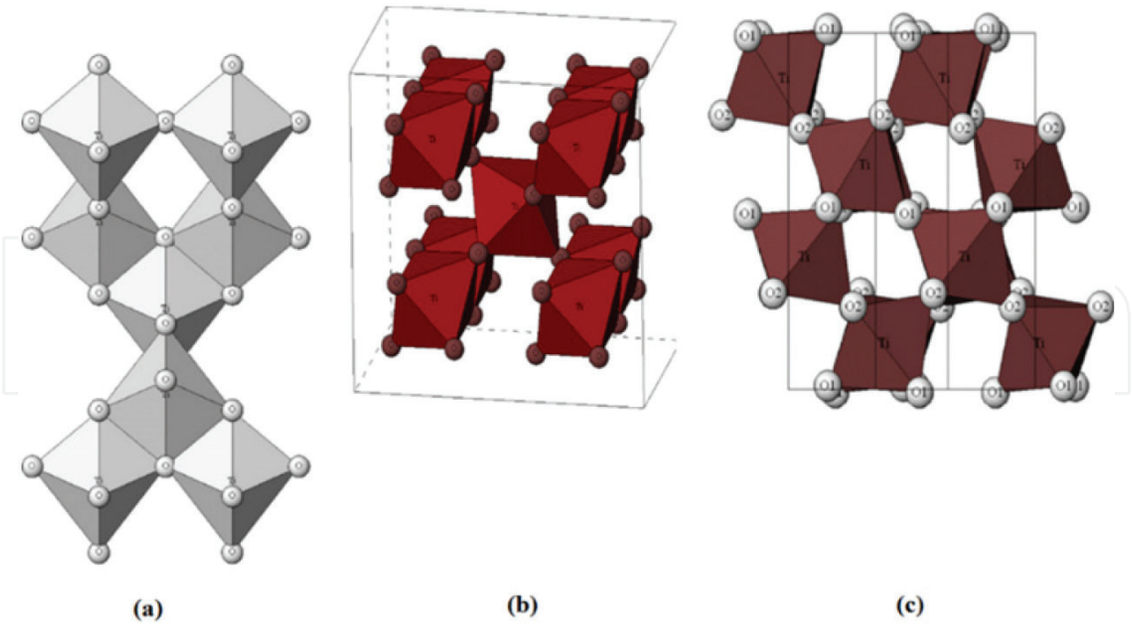

Figure 1. Crystalline structures of titanium dioxide (a) anatase, (b) rutile, and (c) brookite [5].

It is worth to mention, amongst all three different phases of TiO_2, anatase is well-known phase for better photocatalytic performance in various applications, including photocatalytic degradation of organic dye molecules, photocatalytic water splitting and dye-sensitized solar cells compared to other phases [9, 10]. The photocatalytic reaction usually accelerates when a semiconductor interacts with light with enough energy (or a certain wavelength). Two simultaneously reactions occur, including oxidation of dissociative adsorbed H_2O by photogenerated holes and reduction of an electron acceptor by photoexcited electrons. In the photocatalysis process, light energy greater than the bandgap energy is required to transfer photoexcited electrons to the conduction band of semiconductors. **Figure 2** shows that the absorption of photons with enough energy ($\lambda \leq 390$ nm for anatase TiO_2) transfer photoexcited electron to the conduction band ($\bar{e}_{CB}$) and leave a positive hole behind in the valence band (h^+_{VB}) [4, 11]. Many parameters such as size, specific surface area, pore volume, pore structure, crystalline phase, and the exposed surface facets can significantly influence the photocatalytic performance of TiO_2 [2, 10]. It is well known that the photocatalytic applications of TiO_2 are based on the nanoscale materials due to the quantum confinement effects in nanoparticles. Therefore, this effect could change the electron and hole transport behavior and shifts the electronic band structures [7, 12]. However, they also show unavoidable disadvantages such as fast recombination rate of electron and holes, slow charge carriers transfer and high recycling cost [3]. It is noteworthy to mention that effective charge separation can be considered as the most important factor to determine the photocatalytic activities. Construction of one-dimensional nanostructure of TiO_2 photocatalyst like nanowire, nanorod, and nanotube also facilitates charge transportation and promotes charge separation efficiency [1]. The one-dimensional titanium oxide with a large surface area can be used as catalytic carrier and be beneficial in absorbing degradation products [13].

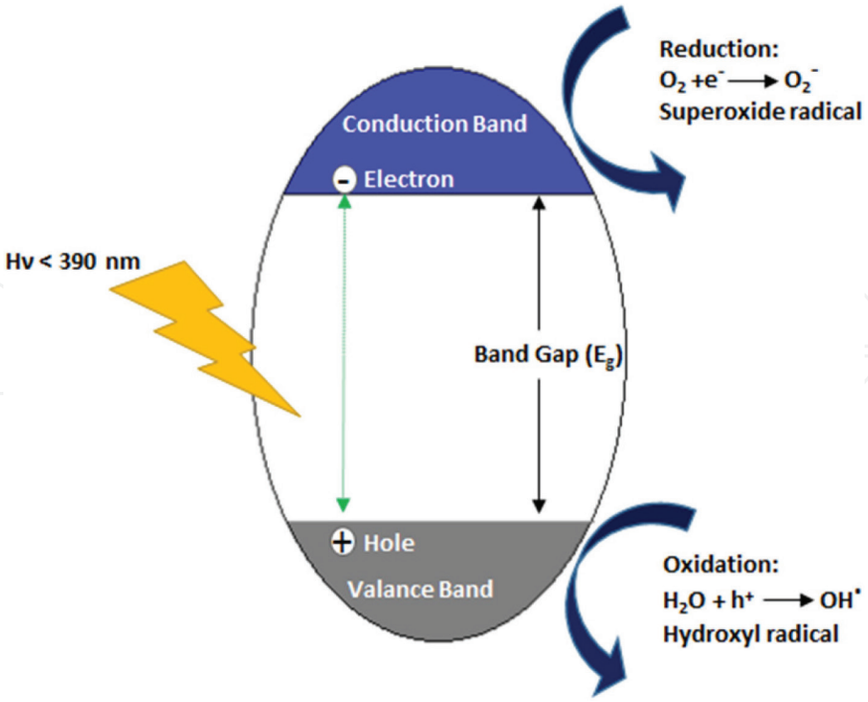

Figure 2. The principle of photocatalytic degradation over TiO_2 photocatalyst [5].

3. Synthesis of 1D-TiO_2 nanostructures

Several methods such as hydrothermal, vapor deposition, sol-gel, and electrospinning, etc. were applied to synthesis various morphologies of 1D-TiO_2 nanostructures like nanotubes, nanorods, nanowires, nanobelts, nanosheets and nanofiber. In this section, we provide the comprehensive information related to hydrothermal method, which is widely used for manufacturing of small particles in the ceramic industry using aqueous or non-aqueous solution.

3.1. Hydrothermal

Hydrothermal is one of the most common methods to synthesis 1D-TiO_2 nanostructure due to simple setup, facile operation, and desirable results. Ever since Kasuga et al. [12] in 1988 showed the first evidence that oxide nanotubes can be obtained easily via chemical treatment, without the need for molds for replication or templates, much research has been carried out on the formation of 1D-TiO_2 nanostructures. In a typical hydrothermal synthesis, TiO_2 or its precursors are dissolved in a concentrated aqueous acidic or alkaline solution and is implemented stainless steel at elevated temperature and pressures [13]. In the former method, the reactants are usually titanium salts with hydrochloric acid and the reaction normally leads to the formation of TiO_2 nanorods. In the latter method, the reactants are TiO_2 nanoparticles and sodium hydroxide solution, which dissolution–recrystallization is always involved in this process and the products include nanotubes, nanowires, and nanobelts. **Figure 3** shows the various morphology of synthesized 1D-TiO_2 nanostructure with hydrothermal method [13–16].

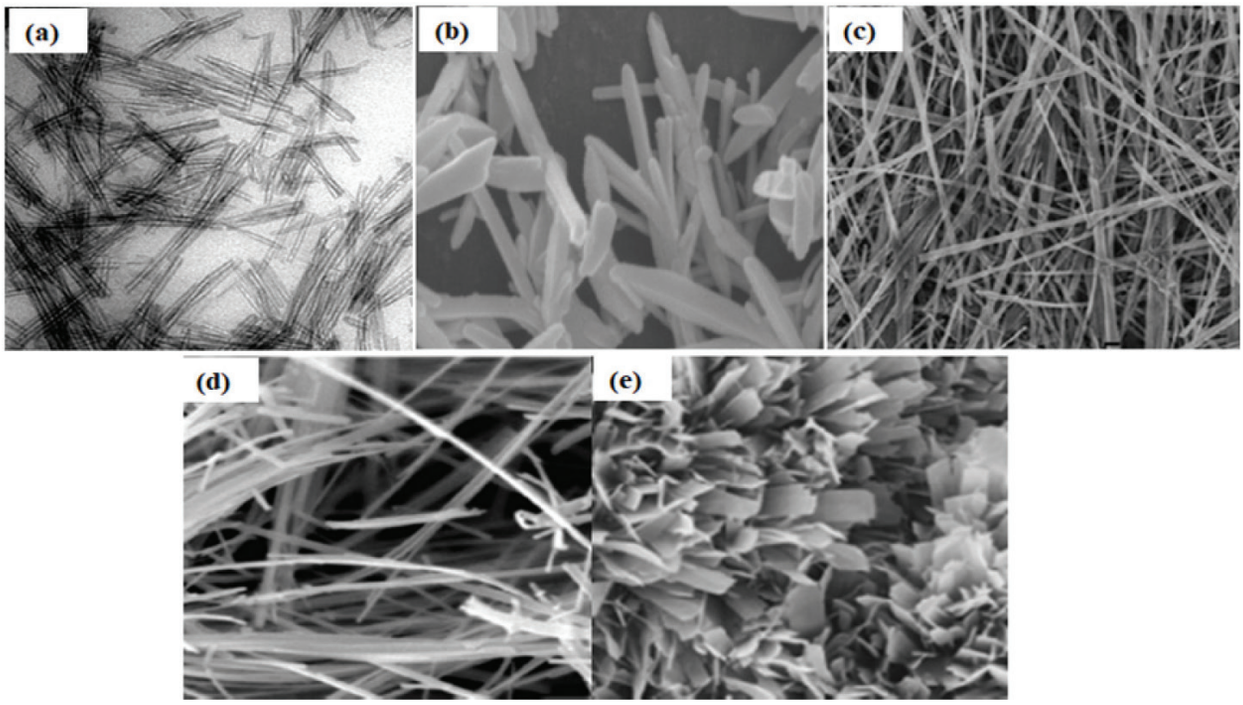

Figure 3. Various morphologies of hydrothermally synthesized 1D-TiO_2 nanostructures: (a) nanotube, (b) nanorods, (c) nanobelts, (d) nanowires, and (e) nanosheets.

Although the synthesis process seems simple, the preparation parameters including the choice of TiO_2 precursors, the hydrothermal condition (temperature, the concentration of reactants and hydrothermal duration), and post washing procedures play important role in the crystal structures and physicochemical properties of 1D-TiO_2 nanostructures [17]. The choice of initial raw materials such as anatase, rutile, brookite, and amorphous TiO_2 may affect the morphology of the resultant 1D-TiO_2 nanostructures but no systematic data is available. Yuan and Su [18] reported the effect of various TiO_2 precursors on the morphology of produced 1D-TiO_2 nanostructures. Crystalline anatase or rutile or commercial P-25 as the raw materials formed titanium oxide nanotubes with diameter 10 nm in the range of reaction temperature of 100–160°C as illustrated in **Figure 4a** [18]. In addition, the surface area of product also affected by raw materials as surface areas of the produced nanotubes from commercial P-25 powder was higher than lab-made anatase TiO_2. It noteworthy to mention that no nanotubes were identified when amorphous TiO_2 powders were the precursor with similar hydrothermal treatment in the presence of NaOH. **Figure 4b** shows that the product morphology was non-tubular needle-shaped fibers morphology in the presence of NaOH with concentration of 5–15 mol/l at the hydrothermal temperature range of 100–160°C. In addition, Nian et al. [19] synthesized anatase TiO_2 nanorods with a specific crystal-elongation direction through hydrothermal treatment of titanate nanotube suspensions under an acidic environment in the absence of surfactants or templates. They suggested that the transformation of the tube to rode is a result of local shrinkage of the tube walls to form anatase crystallites and the subsequent oriented attachment of the crystallites. Furthermore, the hydrothermal temperature strongly controls the morphologies of products. In addition, the increasing of hydrothermal temperature improves yield, length, and degree of crystallinity of nanotubes.

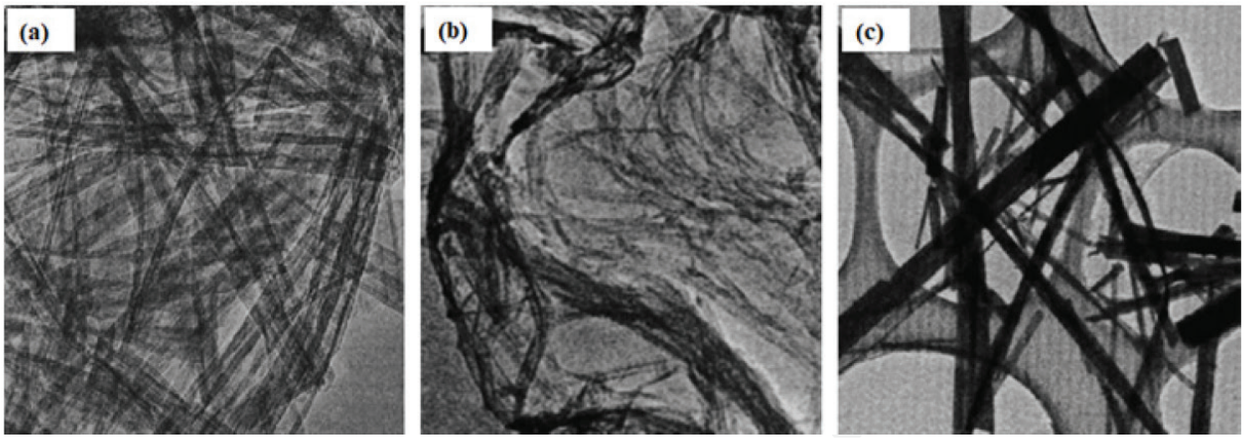

Figure 4. Synthesis of various morphologies of one-dimensional TiO_2 (a) nanotube and (b) nanofiber with crystalline anatase or rutile, amorphous TiO_2, respectively, and (c) effect of increasing hydrothermal temperature on transfer morphology to nanoribbons [18].

The yield of nanotubes increased with the hydrothermal temperature when the temperature was in the range of 100–150°C. The experimental results showed that hydrothermal treatment at below 100°C is not effective to transfer TiO_2 particles and a large amount of residual TiO_2 particles can be found in the product. In another perspective, increasing temperature could facilitate unidirectional crystal growth, leading to different morphologies of 1D-TiO_2 nanostructures. As Yuan et al. reported that crystalline or amorphous TiO_2 powder mainly was transferred to nanoribbons with very high yields (almost 100%) when hydrothermal temperature was in the range of 180–250°C with the NaOH concentration of 5–15 mol/l as shown in **Figure 4c** [18]. Moreover, the hydrothermal treatment duration has a strong effect on the morphological structure of the synthesized product; it also plays a major rule in the conversion of the nanotube structure into nanoribbons as reported by Elsanousi et al. [20]. **Figure 5** shows the effect of hydrothermal treatment duration (5–72 h) at the fixed temperature of 180°C on the morphology of the titanate nanotubes and nanoribbons. The hollow nanotubes were found out with an outer diameter of about 10 nm at treatment duration of 5 and 20 h. While further treatment duration up to 72 h was caused bundles of nanoribbons with widths ranging from 50 to 500 nm and lengths up to several tens of micrometers. Additionally, the experimental results illustrate that there are critical conditions depending on both the treatment duration and varying temperatures (120–195°C), possibly due to a critical pressure, which is needed to be reached so that the transformation process takes place. The concentration and type of alkaline solution also play an important role in the hydrothermal process. The increasing concentration of NaOH can accelerate the hydrothermal reaction owing to the enhancement of Ti (IV) dissolution and exfoliation rates of the precursors. High yield of nanotubes with the maximum surface area of 350 m^2/g can be synthesized with the NaOH concentration between 10 and 15 mol/l. The yield of nanotubes is very low when the NaOH concentration is lower than 5 M or as high as 20 M [18]. Bavykin et al. [21] investigated the influence of the binary NaOH/KOH aqueous mixture used in the hydrothermal process on the morphology of 1D-TiO_2 nanostructures. All observed nanostructures, including nanosheets, nanotubes, nanofibers, and nanoparticles, have been mapped over a wide

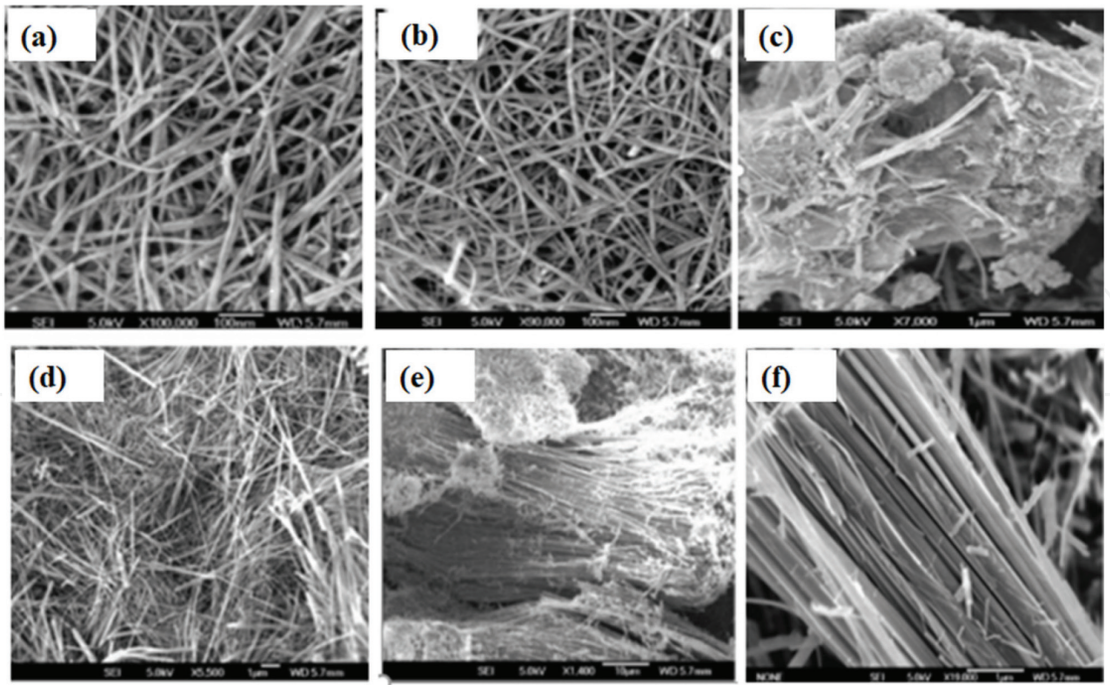

Figure 5. SEM images of the nanotubes and nanoribbons synthesized hydrothermally at 180°C for different durations: (a) 5, (b) 15, (c) 22, (d) 48, and (e and f) 72 h [20].

range of compositions (from pure NaOH to pure KOH) and temperatures (from 50 to 110°C). The hydrothermal process is a cost-effective method with good dispersibility and high purity illustrating the great potential for formation of 1D-TiO_2 nanostructures. However, we cannot ignore its limitations, which diminish its wide applications. For instance, slow reaction kinetics result in long reaction, limited length of the nanotubes, and non-uniformed nanotube for large-scale application.

The coupling hydrothermal treatment with microwave heating, ultrasonication and a rotating autoclave on the reaction mixture can reduce the shortcomings of hydrothermal technique [17, 22].

3.2. Solvothermal method

Solvothermal method facilitates the synthesis of nanometer-sized crystalline TiO_2 powder at relatively low temperatures. Solvothermal reactions are similar to hydrothermal method while a non-aqueous solvent reacts under conditions of high pressure and mild temperature. This method shows promise for developing nanotechnologies. Organic solvents during solvothermal synthesis control the properties of products, corresponding to the structure. The various physical and chemical properties of selected solvent such as reactivity, the polarity, coordinating ability of the solvent, etc. affect the morphology and the crystallization of the final products. Furthermore, the influence of other reaction parameters such as temperature, stirring conditions, and co-solvent (water-ethanol, water-ethylene glycol) on the morphologies of the synthesized nanostructures (nanotubes, nanorods, nanowires, and nanoribbons), as well as their growth mechanism, have been explored [23]. Chen et al. [24] reported the

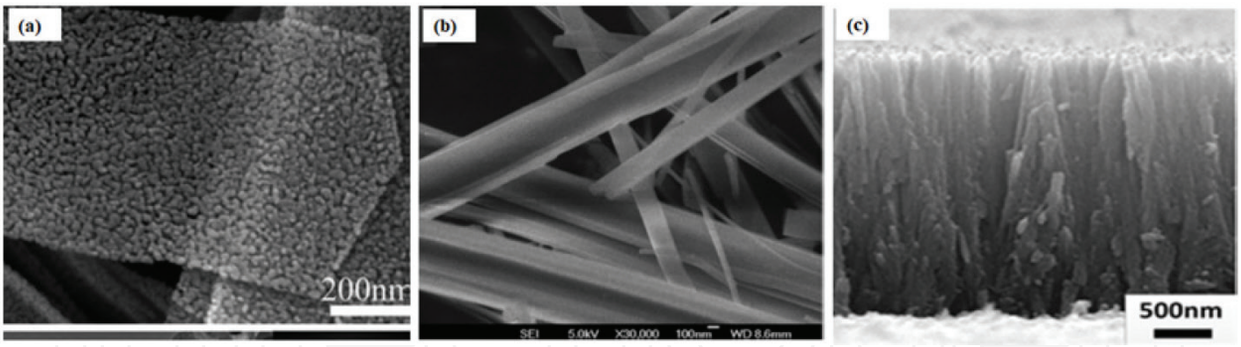

Figure 6. SEM images of various TiO_2 morphologies synthesized by solvothermal method: (a) nanosheets, (b) nanobelts, and (c) nanorods.

preparation of a single-layer polycrystalline anatase TiO_2 (SLP TiO_2) nanosheets **Figure 6a** with a porous structure through a simple solvothermal method by employing, rod-like titanyl sulfate, as the starting material, in the presence of glycerol, followed by a calcination process.

The structure and morphology were found to be dependent on the experimental conditions such as solvothermal reaction time, morphology of titanyl sulfate, and solvent type. Que et al. [25] successfully synthesized the nitrogen-fluorine co-doped TiO_2 nanobelts (**Figure 6b**) with anatase phase structure by the solvothermal method, which employs amorphous titania microspheres as the precursor. Results demonstrate a significantly enhanced photocatalytic degradation of methyl orange compared to commercial TiO_2. Zhao and his co-workers [26] reported the synthesis of TiO_2 nanorod arrays (TNRs) directly on FTO glass (**Figure 6c**) through the solvothermal method, and thermal treatments. The results show that the crystal structure does not change due to thermal treatment. However, the surface morphology appears to change significantly from a thin amorphous layer to tiny crystallite spheres. All of these changes lead to a 39% improvement in the photoelectric conversion efficiency for the nanorod-based photoanode in dye-sensitized solar cells (DSSCs). These findings might be useful in photoelectrical applications of the solvothermal method.

3.3. Other synthesis method

Sol-gel method is another solution-based growth technique, offering several major advantages for mass production of nanomaterials including low-cost, simple processing, and good scalability. This technique is typically conducted through two steps; sol preparation, including mixing the precursors such as metal organic compounds or inorganic metal salts through vigorous stirring to complete hydrolysis and polymerization reaction and gel preparation by removing solvent and converting the sol to a three-dimensional network [27]. This technique is mainly useful for synthesizing oxide ceramic nanomaterials from hydrolyzing titanium precursors. Through sol-gel process, TiO_2 NPs can be aligned following their crystal orientations and form NWs. For example, Rodríguez-Reyes et al. prepared nanocrystalline TiO_2 wires (**Figure 7a–c**) by the sol-gel method, using titanium isopropoxide (TIP) and acetic acid as a TiO_2 sol modifier in alcohol solvent showed to be a successful synthesis route of Ti—O—Ti inorganic network with controlled properties [28].

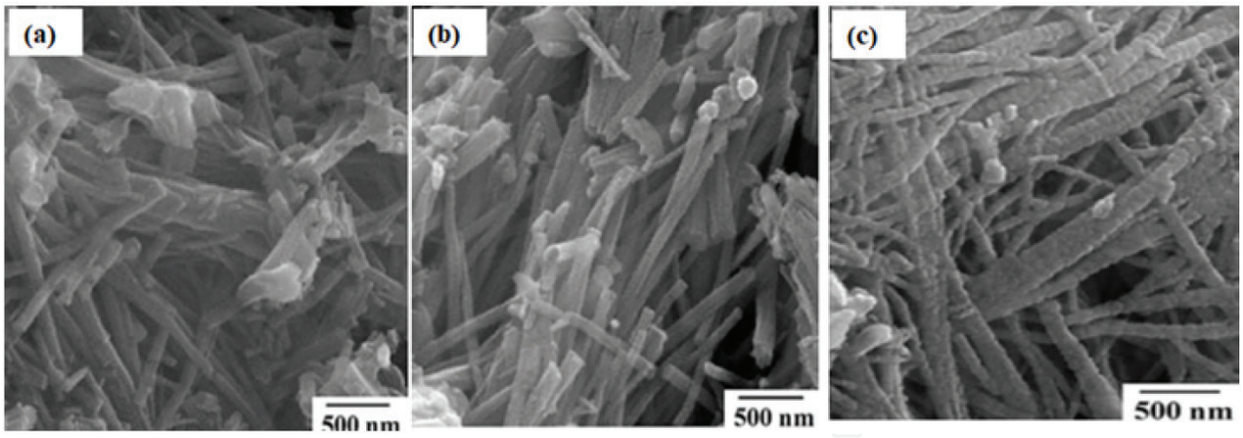

Figure 7. HR-SEM images of TiO_2 calcined at different temperatures (a) 400°C, (b) 500°C, and (c) 600°C [28].

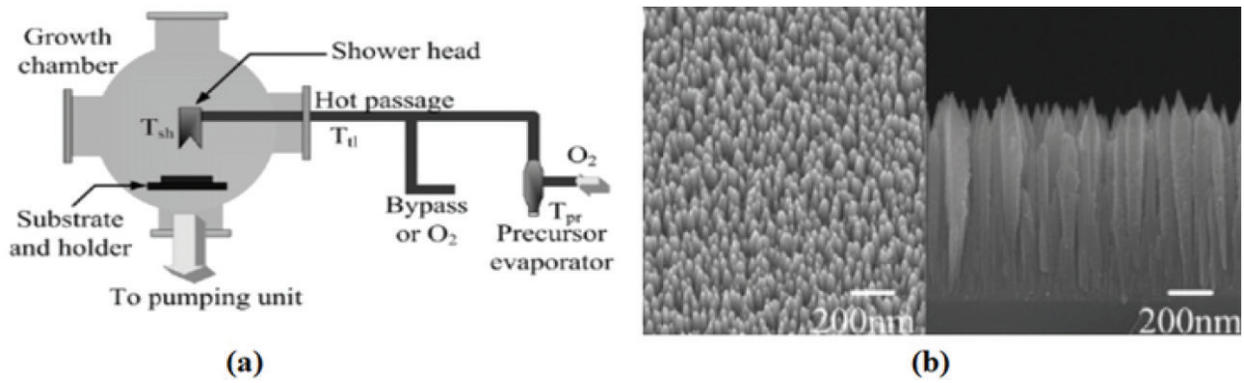

Figure 8. (a) Schematic diagram of the cold wall MOCVD aperture and (b) SEM images of vertically aligned and densely packed TiO_2 NRs grown on sapphire (100) substrate.

The apparent 1-D morphology of TiO_2-related nanowires was thermally stable from 400 to 600°C, showing a similar diameter (about 76 nm); however, crystallite size increases with respect to temperature from 13 to 75 nm.

Vapor deposition method has been developed to high degree of crystallinity 1D-TiO_2 nanostructures (usually single crystal TiO_2) and it can be classified in chemical vapor deposition (CVD) and physical vapor deposition (PVD) [27]. Chen et al. [29] grown well-aligned densely-packed rutile TiO_2 nanorod via metal-organic chemical vapor deposition (MOCVD) (**Figure 8a**), using titanium-tetraisopropoxide (TTIP, $Ti(OC_3H_7)_4$) as a source reagent at a deposition temperature of 550°C and under an oxygen pressure of 1.5 and 5 mbar, respectively. The rutile TiO_2 nanorods (**Figure 8b**) were grown with a very high density and exhibited uniform height. However, this method requires expensive equipment and the cost is too high for mass production.

In addition, nanofibers in different forms, such as core-shell hollow and porous nanofibers are produced with electrospinning method as one of the most conventional methods [30]. These structures of nanofibers can be utilized for new applications such as ultra-filtration, fuel cells, membranes, tissue engineering, catalysis and hydrogen storage. Electrospinning provides

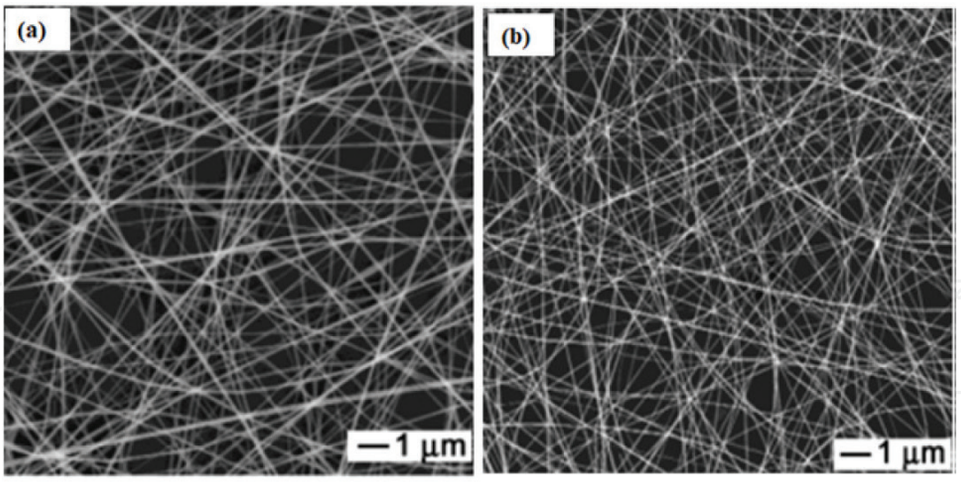

Figure 9. SEM image of TiO_2/PVP nanofibers (a) before calcination and (b) after calcination process at 500°C during 3 h [30].

a straightforward electrohydrodynamical mechanism to produce fibers with diameters less than 100 nm, even up to 5 nm. Under the influence of an electric field, a pendant droplet of the polymer solution at the spinneret is deformed into a conical shape. The post heat treatment is usually needed to remove the solvent and solidify the fiber structures. The viscosity, conductivity, and applied solvents, as well as the conformation and molecular weight of the polymer limit the electrospun ability of a polymer solution. Some polymers are not spinnable because of limited solubility in a proper solvent for electrospinning, having proper polar characteristics [31]. In addition, electrospinning is an efficient method for mass production however; the high resistance caused by the polycrystalline characteristics of the product nanofibers limits its applications. **Figure 9** shows that synthesized anatase nanofibers using electrospinning technique by Li and Xia [30]. They injected ethanol solution including poly(vinyl pyrrolidone) (PVP) and titanium tetraisopropoxide through a needle under a strong electrical field. The final product was the composite nanofibers with lengths up to several centimeters, consisting of PVP and amorphous TiO_2 and followed by calcination process at 500°C. The average diameter of nanofibers was varied from 20 to 200 nm owing to changing a number of parameters like ratio between PVP and titanium tetraisopropoxide, their concentrations in the alcohol solution, the strength of the electric field, and the feeding rate of the precursor solution.

4. Strategies for improving TiO_2 nanostructured photoactivity

As mentioned in the previous sections, 1D-TiO_2 has a wide range of applications, however in this book chapter, we intend to address only the photocatalytic applications including photocatalytic degradation and photocatalytic solar hydrogen production. Nanostructure materials need to meet some requirements for photocatalytic application; (i) should possess a sufficiently large active surface area, (ii) have a broad light absorption band to utilize the full range of solar spectrum, and (iii) should be an effective charge carrier separation to transfer more electron and hole to the interface of the electrode/electrolyte. Nevertheless, there is no

single material, which can match all above criteria [1, 6, 32, 33]. Here, we reviewed the developed strategies on bandgap engineering of titania to extend light absorption into visible light through doping metal and non-metal ions and compositing with another semiconductor for synergic absorption and charge separation for enhanced utilization of solar energy [34].

4.1. Doping with metal and non-metal ions

Incorporation selective doping of metal ion into 1D-TiO_2 nanostructured materials has been proven an efficient route to improve visible light absorption with hindered charge carrier recombination rate. The presence of transition metal ion in the structure of 1D-TiO_2 nanostructured materials increases the formation of Ti^{3+} ions, leading to improve photocatalytic activity, owing to the existence of more oxygen defects, which facilitate the efficient adsorption of oxygen on the titania surface. In addition, the substitution of metal ions into the TiO_2 induces visible light absorption because of introducing intraband state close to the CB or VB edge and charge transfer transition between the **d** electrons of the dopant and the CB (or VB) of TiO_2 nanostructures [34, 35]. Wang et al. [36] investigated the effect of Fe, Mn and Co as dopants on the photoelectrochemical cell performance of TiO_2 nanorods. The maximum photocurrent density of 2.92 mA/cm^2 at 0.25 V vs. Ag/AgCl for Fe/TiO_2, which is five times higher than that of undoped TiO_2 confirmed the presence of Fe into TiO_2 is the most favorable metal to improve the photocatalytic activity of TiO_2 compared to others. **Figure 10a** shows that the photocurrent density of Fe-TiO_2 is as high as 0.96 mA/cm^2 at 0.25 V vs. Ag/AgCl under visible light illumination (>420 nm). Incident-photon-to-current-conversion (IPCE) efficiency (up to 18%) measurements reveal that the Fe-TiO_2 nanorod sample significantly improves the photoresponse not only in the UV region but also in the visible light region, as illustrated in **Figure 10b**.

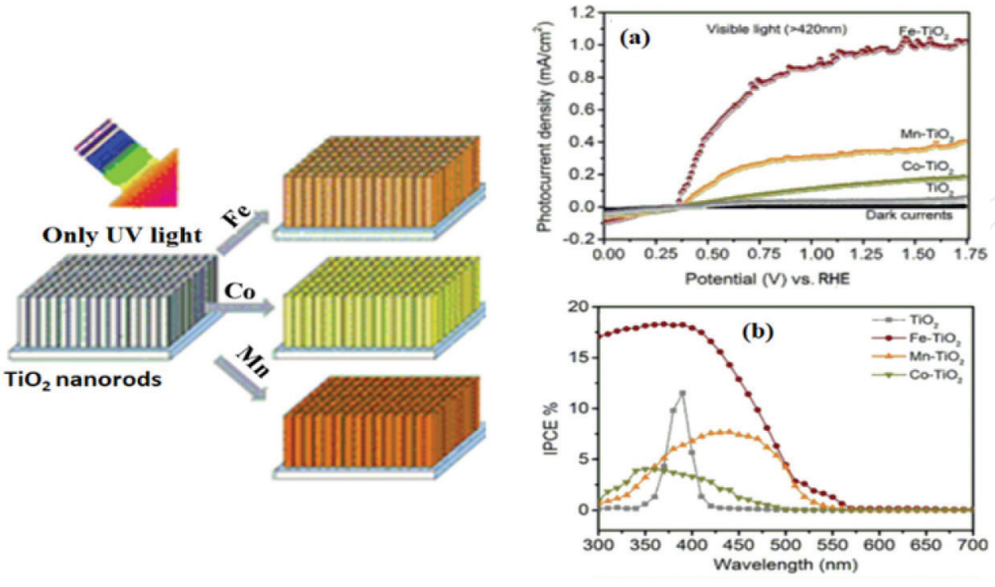

Figure 10. (a) Photocurrent density vs. applied potential curves of four nanorod photoanodes under visible light illumination >420 nm and (b) IPCE spectra of nanorod photoanodes measured at an applied bias of 0.6 V (vs. RHE) in 1 M KOH solution [36].

Moreover, doping non-metal atoms such as nitrogen, sulfur carbon, boron and iodine can extend the absorbance to the visible region and improve the stability of materials through the simple and effective method [37]. For instance, TiO_2/graphene composites were synthesized by Xing et al. [38] through hydrothermal method by decorating Ti^{3+} self-doped TiO_2 nanorods on boron-doped graphene sheets, in which $NaBH_4$ acted as reducing agent and sources of boron dopant on graphene. The produced TiO_2 nanorods had the length of 200 nm with exposed (100) and (010) facets as shown in **Figure 11a**.

The loading of TiO_2 nanorods on graphene sheets was characterized by TEM (**Figure 11b**), and confirmed TiO_2 nanoparticles were covalent bonded to GO, forming a composite favoring the

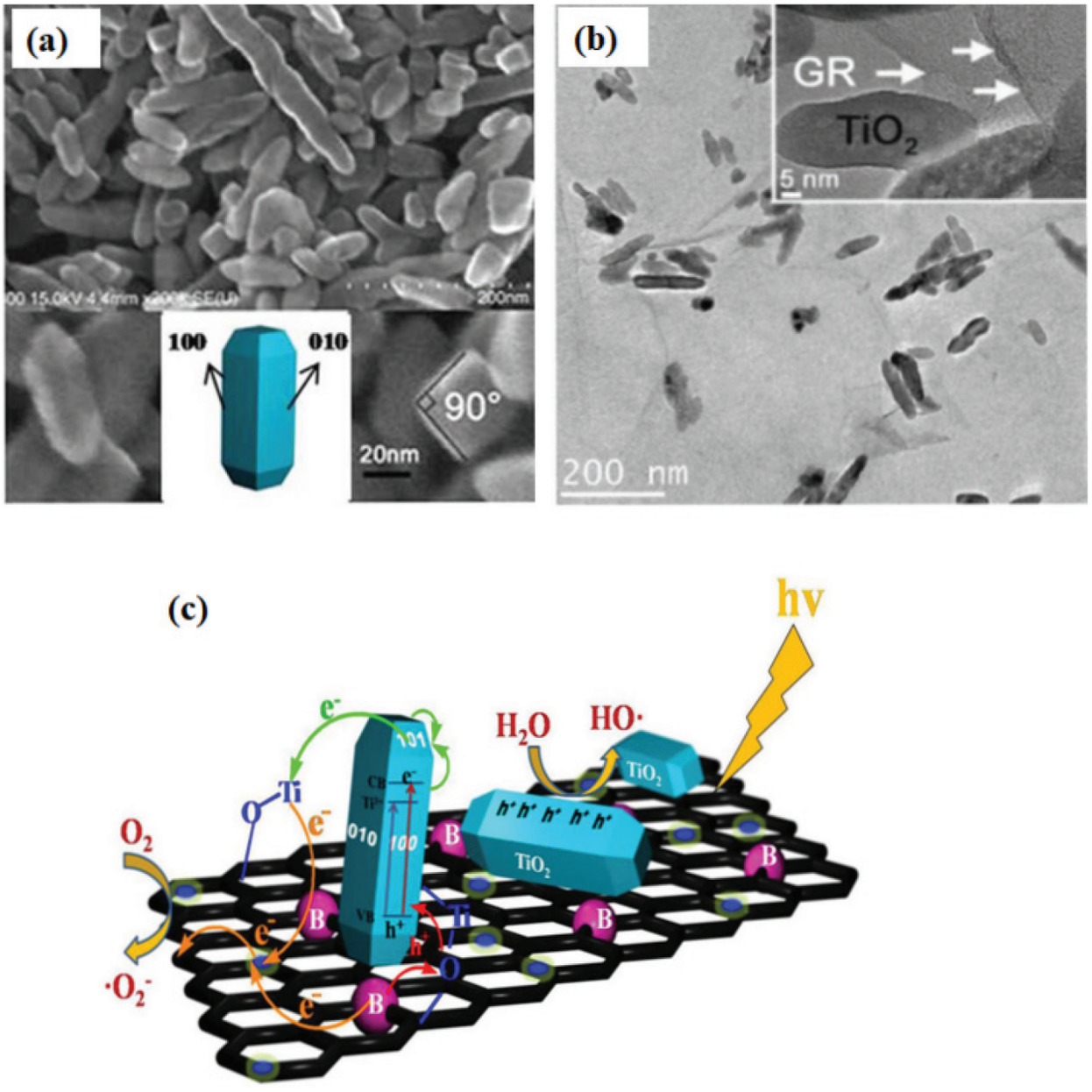

Figure 11. (a) FESEM of TiO_2 nanorods, (b) TEM images of TiO_2/GR composite, and (c) schematic diagram of the charge transfer of TiO_2-x/GR composite [38].

separation of electron-hole pairs (**Figure 11c**). All of the composites tested exhibited improved photocatalytic activities as measured by the degradation of methylene blue and phenol under visible light irradiation. This better photocatalytic activity was attributed to the synergistic effect between Ti^{3+} self-doped TiO_2 and boron-doped graphene.

4.2. Coupling TiO_2 with semiconductors

The fabrication, design, and tailoring of coupling other semiconductors like CdS, Cu_2O, CdSe, WO_3, etc. with 1D-TiO_2 nanostructures to achieve better charge carrier separation in a light energy conversion system have received significant attentions. The charge transfer from one semiconductor to another with suitable band edge positions is thermodynamically favorable to increase the lifetime of the charge carriers thus promoting the interfacial charge transfer and catalytic efficiency [34, 39]. Zhu et al. [39] deposited CdS on TiO_2 nanotube arrays (TNTAs) by successive ionic layer adsorption and reaction (SILAR) method for visible-light-driven hydrogen production and organic compound degradation. CdS has narrow bandgap (~2.40 eV) and relatively high visible absorption coefficient of CdS enables its highly desirable use in solar applications. Coupling CdS with TiO_2 can hamper electron-hole recombination that dominating the charge separation. **Figure 10** shows the schematic diagram of charge transfer in CdS-TNTAs photocatalyst for visible-light photocatalysis. Therefore, this charge transfer can accelerate the separation of charge carriers and enhance the visible-light response and photocatalytic activity for H_2 generation and Rh B degradation of CdS-TNTAs.

5. Applications of 1D-TiO_2 nanostructures

TiO_2 nanostructured materials are widely used as photocatalysts due to its high oxidation and reduction ability. 1D-TiO_2 nanostructures have been paid much attention to photocatalytic degradation of pollutants, photocatalytic CO_2 reduction into energy fuels, photocatalytic water splitting, solar cells, supercapacitors and lithium batteries. This section is dedicated to the application of 1D-TiO_2 nanostructures in photocatalytic water splitting and dye sensitized solar cells (**Figure 12**).

5.1. Dye sensitized solar cell

The first sensitization of large bandgap energy toward the visible region was reported in 1972 with ZnO semiconductor with the photoconversion efficiency of 1–2.5%. Gratzel et al. reported a breakthrough in the efficiency over 7% in 1991 using large surface area nano-crystalline TiO_2 thin film, sensitizing with ruthenium complex. They explained that high surface area of TiO_2 helps to better absorb and attach dye on the surface of TiO_2 thin film [40, 41]. **Figure 13a** and **b** displays a schematic presentation of DSSC and its operation principle. It includes nano-crystalline TiO_2 thin film as a working electrode (WE) or photoanode with a monolayer of sensitizer in contact with iodide/tri-iodide redox electrolyte, which is sandwiched by second conductive glass covered with platinum as a counter electrode (CE). The most efficient DSSC had the highly mesoporous of anatase phase of TiO_2 which was coated on the surface of FTO (F-doped tin oxide) glass substrate with thickness 5–20 μm and covered

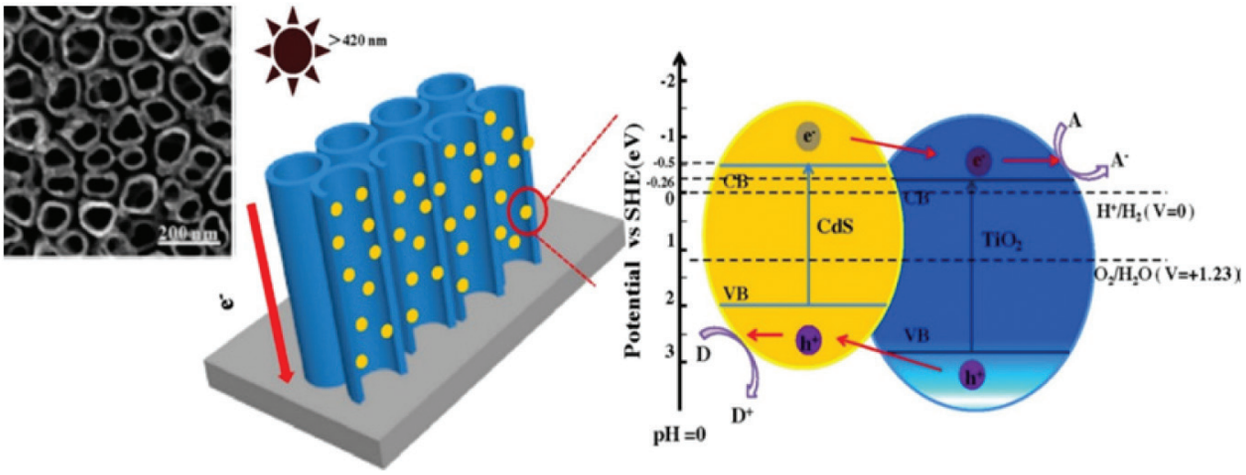

Figure 12. SEM image and schematic diagram of charge transfer in CdS-TNTAs photocatalyst for visible-light photocatalysis [39].

by a monolayer of sensitizer. To overcome the drawback of TiO_2 nanoparticles, a 1D-TiO_2 nanostructure is often applied as photoanode to enhance electron transfer ability. **Figure 14a** shows a novel TiO_2 nanoparticles and TiO_2 nanotube (TNP/TNA) multilayer photoelectrode via a layer-by-layer assembly process to improve the DSSC performance as reported by Yang et al. [42]. The fabricated DSSC with multilayer photoelectrode has higher efficiency than the single-layer or bare DSSCs. The TNP/TNA four-layer photoelectrode provided a large surface area for dye adsorption with the highest photocurrent density (**Figure 14b**) and maximum photoconversion efficiency of 7.22% because of effective electron transport.

5.2. Photocatalytic solar hydrogen production

Energy dense fossil fuels are non-renewable source and the most coveted fuel that have ever been discovered, burning fossil fuels release such significant amount of greenhouse gases in

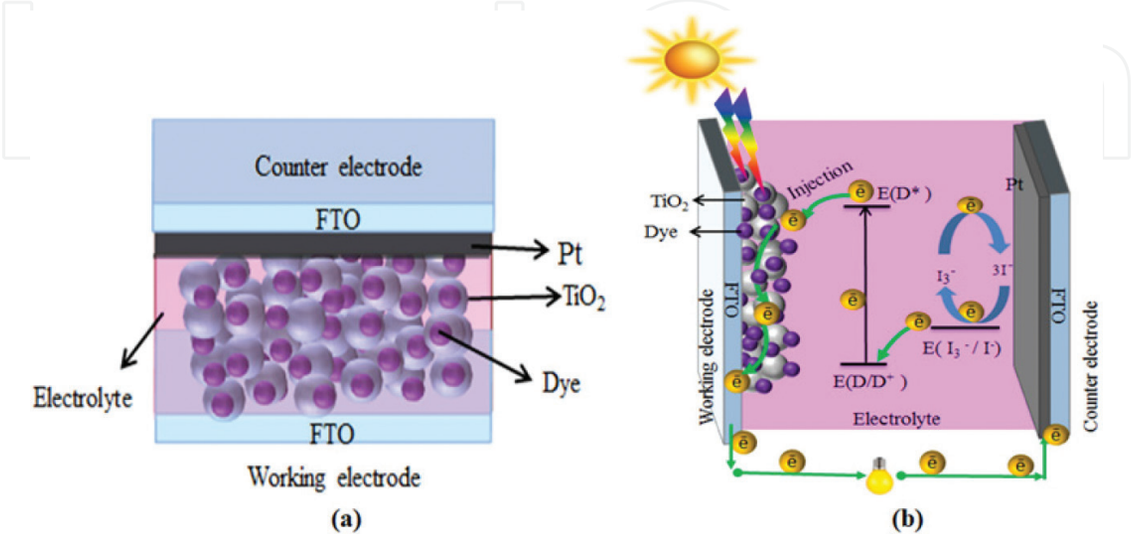

Figure 13. (a) Schematic diagram and (b) principle of operation and energy level of DSSC.

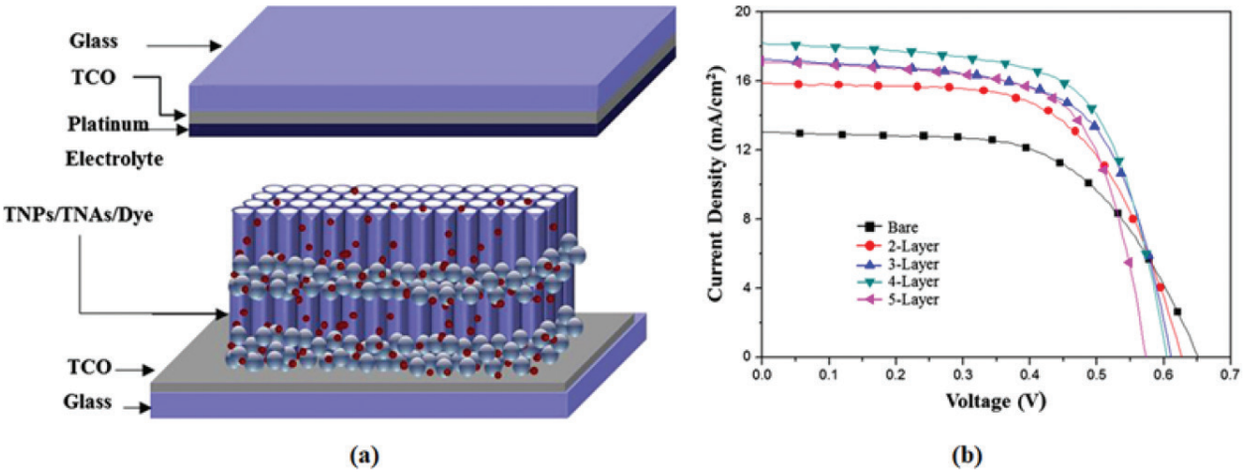

Figure 14. (a) Structure of multilayer DSSC and (b) I-V curves of DSSC with single to five-layer photoelectrodes [42].

the atmosphere as major threats to the environment and human health. Hydrogen has been established as a clean energy carrier in many applications such as automotive, domestic heating, aircrafts and stationary power generation. Utilizing solar energy to split water into H_2 and O_2 in photoelectrochemical (PEC) cell is in fact one of the most promising technologies for hydrogen production. It would be interesting to combine solar energy and water in PEC cell to produce truly renewable and low environmental impact fuel on both large and small scale. A photocatalyst is the core of this system with some requirements like an optimal bandgap energy approximately 2 eV and a sufficient negative CB position [6]. Up to date, there has not been found any photocatalyst that meets all requirements for hydrogen production in the PEC cell. Amongst different metal oxide photocatalysts, TiO_2 is an attractive n-type photocatalyst in terms of hydrogen production regardless of its limitations [43, 44]. The vertically oriented 1D-TiO_2 nanostructure are promising materials for photocatalytic solar hydrogen production due to their impressive vectorial 1D-channel pathways for fast electron transport in the axial direction. Shinde et al. [45] synthesized nanocomposite heterojunction photoanode involving

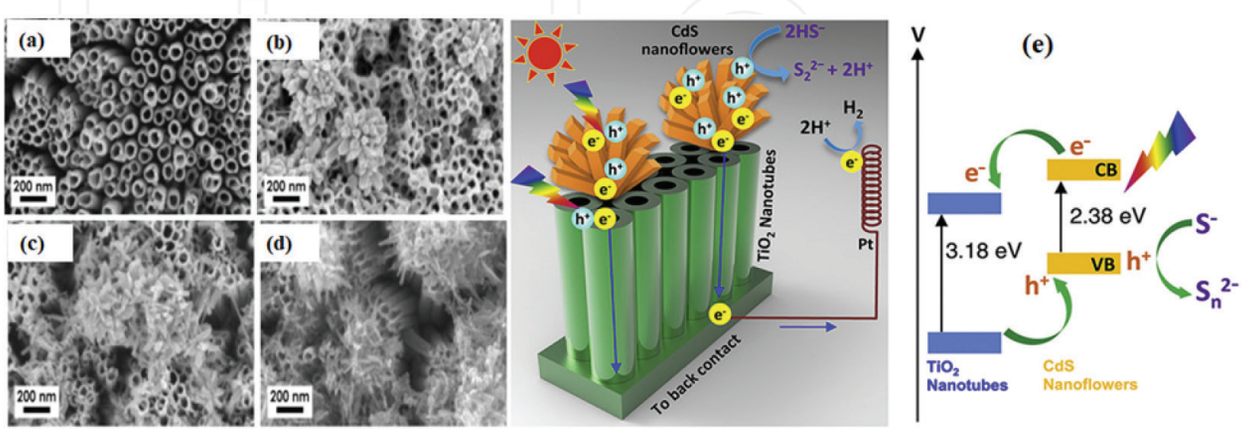

Figure 15. Surface FESEM images of (a) annealed TiO_2NT photoanode and CdS-NF/TiO_2-NT photoanodes prepared with different annealing conditions: (b) as-grown CdS on as-grown TiO_2 NT array, (c) as-grown CdS on annealed TiO_2 NT array, (d) annealed CdS on annealed TiO_2 NT array, and (e) the schematic of charge transfer mechanism in heterojunction of CdS NFs and TiO_2 NT array [45].

CdS nanoflowers (NFs) and one-dimensional TiO_2 nanotube (TNT) arrays. An anodization method was employed for fabrication of TiO_2 nanotube (TNT) arrays and CdS NFs was decorated on the surface of TNT using hydrothermal method as shown in **Figure 15a–d**. As-grown CdS-NF/TiO_2-NT array photoanode exhibited a 5.5-fold photocurrent enhancement in a polysulfide electrolyte compared to the pristine TiO_2 NT photoanode. Annealing of TiO_2 NTs as well as CdS NFs led to further improvement in the photocurrent owing to greater crystallinity, significantly higher visible light photon absorption and improved interface properties between CdS and TiO_2. The better photocatalytic performance of CdS-NF/TiO_2-NT was attributed to effective absorption of the visible light photons, leading to the photo-generation of electron-hole pairs and greater charge carrier separation as shown in **Figure 15e**.

6. Conclusion

Over recent decades, the tremendous efforts have been paid to develop TiO_2 nanomaterials and large amount of information provided on their synthesis, modification, and applications. The one-dimensional TiO_2 nanostructures have been comprehensively studied due to its distinctive advantages with regard to less charge carrier recombination rates and unique physical and chemical properties. In this chapter, we first explain the structural features of the three TiO_2 polymorphs that have been seen in TiO_2 nanostructures. Then, the various synthesis processes of one-dimensional TiO_2 nanostructures were discussed. Hydro/solvothermal method and the effect of the experimental parameters on the formation of various morphologies and properties of 1D-TiO_2 nanostructures were thoroughly reviewed. In addition, we studied some strategies on bandgap engineering of titania to improve optical properties and charge carrier separation and transfer to the surface of photocatalyst. Finally, the applications of 1D-TiO_2 nanostructures in photocatalytic water splitting and dye-sensitized solar cells have been reported with regard to their specific structure and properties. Therefore, these data favorable for further investigation on the development of sustainable environmental remediation and energy technologies based the photocatalytic process by driving solar light as renewable source of energy.

Author details

Norani Muti Mohammed[1], Robabeh Bashiri[1]*, Suriati Sufian[2], Chong Fai Kait[3] and Saeed Majidai[4]

*Address all correspondence to: robabeh.bashiri@utp.edu.my

1 Centre of Innovative Nanostructures and Nanodevices (COINN), Universiti Teknologi PETRONAS, Perak, Malaysia

2 Chemical Engineering Department, Universiti Teknologi PETRONAS, Perak, Malaysia

3 Fundamental and Applied Sciences Department, Universiti Teknologi PETRONAS, Perak, Malaysia

4 Leap Energy Partners, Kuala Lumpur, Malaysia

References

[1] Tian J, Zhao Z, Kumar A, Boughton RI, Liu H. Recent progress in design, synthesis, and applications of one-dimensional TiO_2 nanostructured surface heterostructures: A review. Chemical Society Reviews. 2014;**43**(20):6920-6937. DOI: 10.1039/C4CS00180J

[2] Nakata K, Fujishima A. TiO_2 photocatalysis: Design and applications. Journal of Photochemistry and Photobiology C: Photochemistry Reviews. 2012;**13**(3):169-189. DOI: 10.1016/j.jphotochemrev.2012.06.001

[3] Ge M, Cao C, Huang J, Li S, Chen Z, Zhang KQ, Al-Deyab SS, Lai Y. A review of one-dimensional TiO_2 nanostructured materials for environmental and energy applications. Journal of Materials Chemistry A. 2016;**4**(18):6772-6801. DOI: 10.1039/C5TA09323F

[4] Bashiri R, Mohamed NM, Kait CF, Sufian S, Khatani M. Enhancing photoelectrochemical hydrogen production over Cu and Ni doped titania thin film: Effect of calcination duration. Journal of Environmental Chemical Engineering. 2017;**5**(4):3207-3214. DOI: 10.1016/j.jece.2017.06.027

[5] Pelaez M, Nolan NT, Pillai SC, Seery MK, Falaras P, Kontos AG, Dunlop PSM, Hamilton JWJ, Byrne JA, O'Shea K, Entezari MH, Dionysiou DD. A review on the visible light active titanium dioxide photocatalysts for environmental applications. Applied Catalysis B: Environmental. 2012;**125**:331-349. DOI: 10.1016/j.apcatb.2012.05.036

[6] Bashiri R, Mohamed NM, Kait CF. Advancement of sol-gel–prepared TiO_2 photocatalyst. In: Chandra U, editor. Recent Applications in Sol-Gel Synthesis. Rijeka: InTech; 2017. pp. 151-167

[7] Bashiri R, Mohamed NM, Kait CF, Sufian S. Hydrogen production from water photosplitting using Cu/TiO_2 nanoparticles: Effect of hydrolysis rate and reaction medium. International Journal of Hydrogen Energy. 2015;**4**(18):6021-6037. DOI: 10.1016/j.ijhydene.2015.03.019

[8] Samsudin MFR, Sufian S, Mohamed NM, Bashiri R, Wolfe F, Ramli RM. Enhancement of hydrogen production over screen-printed $TiO_2/BiVO_4$ thin film in the photoelectrochemical cells. Materials Letters. 2018;**211**(Supplement C):13-16. DOI: 10.1016/j.matlet.2017.09.013

[9] Yang S, Huang N, Jin YM, Zhang HQ, Su YH, Yang HG. Crystal shape engineering of anatase TiO_2 and its biomedical applications. CrystEngComm. 2015;**17**(35):6617-6631. DOI: 10.1039/C5CE00804B

[10] Bashiri R, Mohamed NM, Kait CF, Sufian S, Kakooei S, Khatani M, Gholami Z. Optimization hydrogen production over visible light-driven titania-supported bimetallic photocatalyst from water photosplitting in tandem photoelectrochemical cell. Renewable Energy. 2016;**99**:960-970. DOI: 10.1016/j.renene.2016.07.079

[11] Liu J, Yu X, Liu Q, Liu R, Shang X, Zhang S, Li W, Zheng W, Zhang G, Cao H, Gu Z. Surface-phase junctions of branched TiO_2 nanorod arrays for efficient photoelectrochemical water splitting. Applied Catalysis B: Environmental. 2014;**158-159**:296-300. DOI: 10.1016/j.apcatb.2014.04.032

[12] Kasuga T, Hiramatsu M, Hoson A, Sekino T, Niihara K. Formation of titanium oxide nanotube. Langmuir. 1998;**14**(12):3160-3163. DOI: 10.1021/la9713816

[13] Liu N, Chen X, Zhang J, Schwank JW. A review on TiO_2-based nanotubes synthesized via hydrothermal method: Formation mechanism, structure modification, and photocatalytic applications. Catalysis Today. 2014;**225**(Supplement C):34-51. DOI: 10.1016/j.cattod.2013.10.090

[14] Chen J, Yang HB, Miao J, Wang H-Y, Liu B. Thermodynamically driven one-dimensional evolution of anatase TiO_2 nanorods: One-step hydrothermal synthesis for emerging intrinsic superiority of dimensionality. Journal of the American Chemical Society. 2014;**136**(43):15310-15318. DOI: 10.1021/ja5080568

[15] Zhou W, Du G, Hu P, Li G, Wang D, Liu H, Wang J, Boughton RI, Liu D, Jiang H. Nanoheterostructures on TiO_2 nanobelts achieved by acid hydrothermal method with enhanced photocatalytic and gas sensitive performance. Journal of Materials Chemistry. 2011;**21**(22):7937-7945. DOI: 10.1039/C1JM10588D

[16] Zhang X, Li D, Wan J, Yu X. Hydrothermal synthesis of TiO_2 nanosheets photoelectrocatalyst on Ti mesh for degradation of norfloxacin: Influence of pickling agents. Materials Science in Semiconductor Processing. 2016;**43**(Supplement C):47-54. DOI: 10.1016/j.mssp.2015.11.020

[17] Zhou W, Liu H, Boughton RI, Du G, Lin J, Wang J, Liu D. One-dimensional single-crystalline Ti-O based nanostructures: Properties, synthesis, modifications and applications. Journal of Materials Chemistry. 2010;**20**(29):5993-6008. DOI: 10.1039/B927224K

[18] Yuan Z-Y, Su B-L. Titanium oxide nanotubes, nanofibers and nanowires. Colloids and Surfaces A: Physicochemical and Engineering Aspects. 2004;**241**(1):173-183. DOI: 10.1016/j.colsurfa.2004.04.030

[19] Nian J-N, Teng H. Hydrothermal synthesis of single-crystalline anatase TiO_2 nanorods with nanotubes as the precursor. The Journal of Physical Chemistry B. 2006;**110**(9):4193-4198

[20] Elsanousi A, Elssfah EM, Zhang J, Lin J, Song HS, Tang C. Hydrothermal treatment duration effect on the transformation of titanate nanotubes into nanoribbons. The Journal of Physical Chemistry C. 2007;**111**(39):14353-14357. DOI: 10.1021/jp074566m

[21] Bavykin DV, Kulak AN, Walsh FC. Metastable nature of titanate nanotubes in an alkaline environment. Crystal Growth & Design. 2010;**10**(10):4421-4427. DOI: 10.1021/cg100529y

[22] Ge M, Li Q, Cao C, Huang J, Li S, Zhang S, Chen Z, Zhang K, Al-Deyab SS, Lai Y. One-dimensional TiO_2 nanotube photocatalysts for solar water splitting. Advanced Science. 2017;**4**(1):1600152. DOI: 10.1002/advs.201600152

[23] Nam CT, Falconer JL, Duc LM, Yang W-D. Morphology, structure and adsorption of titanate nanotubes prepared using a solvothermal method. Materials Research Bulletin. 2014;**51**(Supplement C):49-55. DOI: 10.1016/j.materresbull.2013.11.036

[24] Chen Y, Tian G, Ren Z, Tian C, Pan K, Zhou W, Fu H. Solvothermal synthesis, characterization, and formation mechanism of a single-layer anatase TiO_2 nanosheet with a porous structure. European Journal of Inorganic Chemistry. 2011;**2011**(5):754-760. DOI: 10.1002/ejic.201000999

[25] He Z, Que W, Chen J, Yin X, He Y, Ren J. Photocatalytic degradation of methyl orange over nitrogen–fluorine codoped TiO_2 nanobelts prepared by solvothermal synthesis. ACS Applied Materials & Interfaces. 2012;**4**(12):6816-6826. DOI: 10.1021/am3019965

[26] Zhao J, Yao J, Zhang Y, Guli M, Xiao L. Effect of thermal treatment on TiO_2 nanorod electrodes prepared by the solvothermal method for dye-sensitized solar cells: Surface reconfiguration and improved electron transport. Journal of Power Sources. 2014;**255**:16-23. DOI: 10.1016/j.jpowsour.2013.12.127

[27] Wang X, Li Z, Shi J, Yu Y. One-Dimensional Titanium Dioxide Nanomaterials: Nanowires, Nanorods, and Nanobelts. Vol. 1142014

[28] Rodríguez-Reyes M, Dorantes-Rosales HJ. A simple route to obtain TiO_2 nanowires by the sol-gel method. Journal of Sol-Gel Science and Technology. 2011;**59**(3):658. DOI: 10.1007/s10971-011-2541-5

[29] Chen CA, Chen YM, Korotcov A, Huang YS, Tsai DS, Tiong KK. Growth and characterization of well-aligned densely-packed rutile TiO_2 nanocrystals on sapphire substrates via metal–organic chemical vapor deposition. Nanotechnology. 2008;**19**(7):075611

[30] Li D, Xia Y. Fabrication of titania nanofibers by electrospinning. Nano Letters. 2003; **3**(4):555-560. DOI: 10.1021/nl034039o

[31] Khajavi R, Abbasipour M. Electrospinning as a versatile method for fabricating coreshell, hollow and porous nanofibers. Scientia Iranica. 2012;**19**(6):2029-2034. DOI: 10.1016/j.scient.2012.10.037

[32] Bashiri R, Mohamed NM, Fai Kait C, Sufian S. Influence of hydrolysis rate on properties of nanosized TiO_2 synthesized via sol-gel hydrothermal. In: Advanced Materials Research. Trans Tech Publ.; 2015

[33] Norani MM, Bashiri R, Chong FK, Sufian S, Kakooei S. Photoelectrochemical behavior of bimetallic Cu–Ni and monometallic Cu, Ni doped TiO_2 for hydrogen production. International Journal of Hydrogen Energy. 2015;**40**(40):14031-14038. DOI: 10.1016/j.ijhydene.2015.07.064

[34] Kumar SG, Devi LG. Review on modified TiO_2 photocatalysis under UV/visible light: Selected results and related mechanisms on interfacial charge carrier transfer dynamics. The Journal of Physical Chemistry A. 2011;**115**(46):13211-13241. DOI: 10.1021/jp204364a

[35] Bashiri R, Mohamed NM, Kait CF, Sufian S, Khatani M, Hanaei H. Effect of preparation parameters on optical properties of Cu and Ni doped TiO_2 photocatalyst. Procedia Engineering. 2016;**148**:151-157. DOI: 10.1016/j.proeng.2016.06.506

[36] Wang C, Chen Z, Jin H, Cao C, Li J, Mi Z. Enhancing visible-light photoelectrochemical water splitting through transition-metal doped TiO_2 nanorod arrays. Journal of Materials Chemistry A. 2014;**2**(42):17820-17827. DOI: 10.1039/C4TA04254A

[37] Szkoda M, Siuzdak K, Lisowska-Oleksiak A. Non-metal doped TiO_2 nanotube arrays for high efficiency photocatalytic decomposition of organic species in water. Physica E: Low-Dimensional Systems and Nanostructures. 2016;**84**(Supplement C):141-145. DOI: 10.1016/j.physe.2016.06.004

[38] Xing M, Li X, Zhang J. Synergistic effect on the visible light activity of Ti^{3+} doped TiO_2 nanorods/boron doped graphene composite. Scientific Reports. 2014;**4**:5493 https://www.nature.com/articles/srep05493#supplementary-information

[39] Zhu Y, Wang Y, Chen Z, Qin L, Yang L, Zhu L, Tang P, Gao T, Huang Y, Sha Z, Tang G. Visible light induced photocatalysis on CdS quantum dots decorated TiO_2 nanotube arrays. Applied Catalysis A: General. 2015;**498**(Supplement C):159-166. DOI: 10.1016/j.apcata.2015.03.035

[40] Baraton M-I. Nano-TiO_2 for solar cells and photocatalytic water splitting: Scientific and technological challenges for commercialization. The Open Nanoscience Journal. 2011;**5**(1):64-77

[41] Boercker JE. Synthesis of Titanium Dioxide and Zinc Oxide Nanowires for Excitonic Solar Cells. Faculty of the Graduate School; 2009. p. 204

[42] Yang JH, Kim KH, Bark CW, Choi HW. The effect of dye-sensitized solar cell based on the composite layer by anodic TiO_2 nanotubes. Nanoscale Research Letters. 2014;**9**(1):671. DOI: 10.1186/1556-276x-9-671

[43] Naseri N, Kim H, Choi W, Moshfegh AZ. Optimal Ag concentration for H_2 production via Ag:TiO_2 nanocomposite thin film photoanode. International Journal of Hydrogen Energy. 2012;**37**(4):3056-3065. DOI: 10.1016/j.ijhydene.2011.11.041

[44] Sreethawong T, Laehsalee S, Chavadej S. Comparative investigation of mesoporous- and non-mesoporous-assembled TiO_2 nanocrystals for photocatalytic H_2 production over N-doped TiO_2 under visible light irradiation. International Journal of Hydrogen Energy. 2008;**33**(21):5947-5957. DOI: 10.1016/j.ijhydene.2008.08.007

[45] Shinde PS, Park JW, Mahadik MA, Ryu J, Park JH, Yi Y-J, Jang JS. Fabrication of efficient CdS nanoflowers-decorated TiO_2 nanotubes array heterojunction photoanode by a novel synthetic approach for solar hydrogen production. International Journal of Hydrogen Energy. 2016;**41**(46):21078-21087. DOI: 10.1016/j.ijhydene.2016.08.205